19TH INTERNATIONAL COSMIC RAY CONFERENCE

LA JOLLA, USA AUGUST 11-23, 1985

CONFERENCE PAPERS

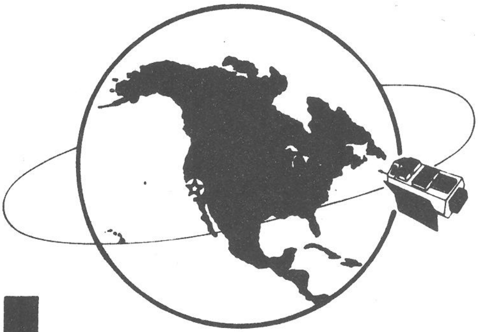

SH

SESSIONS
VOL. 4

STUDY OF NON-THERMAL PHOTON PRODUCTION UNDER DIFFERENT SCENARIOS IN SOLAR FLARES. II. THE COMPTON INVERSE AND BREMSSTRAHLUNG MODELS AND FITTINGS.

J. Pérez-Peraza* and M. Alvarez*;A. Laville**
Instituto de Geofísica UNAM, 04510-C.U., México, D. F., MEXICO

A.Gallegos
Depto. de Física, UPICSA, 08400 - México, D. F., MEXICO

1. Introduction. Energy spectra of photons emitted from Bremsstrahlung (BR) of energetic electrons with matter, is obtained from the deconvolution of the electron energy spectra derived in SH 1.2.-2. According to Kane and Anderson (1970), the differential photon flux at the earth level is

$$\frac{dJ(h\nu)}{d(h\nu)} = \frac{3.53\times10^{-28}E.M.}{n}\int_{E}^{E_m}\frac{d\sigma(E,h\nu)}{dE}N(E)dE \quad (\text{photons/s KeV cm}^2) \qquad [1]$$

where $d\sigma(E,h\nu)/dE$ is the differential cross-section for electron-proton (BR), given in the non-relativistic range by the Bethe-Heitler formula (Jackson, 1962) and in the relativistic domain by the Koch and MQtz formula (Bai and Ramaty, 1976); $E.M. = n^2V$ is the emission measure, with n and V the number density and volume respectively. For Inverse Compton (IC) we followed Sheng (1972), introducing $\sigma(W,h\nu) = \sigma_t\delta[h\nu-(4/3)\bar{\varepsilon}(W/m_ec^2)^2]$ in eq.(1) for $W<(m_ec^2)^2/4\bar{\varepsilon}\sim 290$ MeV, where W=total electron energy, $\sigma_t=6.65\times10^{-25}$ cm^2=Thompson cross-section and $\bar{\varepsilon}=2.7kT$= mean thermal photon energy, and we obtained at 1 Astronomical Unit.

$$dJ(h\nu)/d(h\nu)=(4.39\times10^{-31}\ E.M.\omega_{ph}(h\nu)^{\frac{1}{2}}/n^2T^{3/2})N(E=m_ec^2\{(3h\nu/4\bar{\varepsilon})^{\frac{1}{2}}-1\}) \quad (\text{photons/s KeV cm}^2) \qquad [2]$$

For the evaluation of the electron energy spectra we have explored different combinations of the source physical parameter in the scenarios displayed in SH 1.2-2: $n=10^{10}-10^{13}$ cm^{-3} with $T=10^5-10^7$ °K in scenario (a), $n=10^{10}-10^{12}$ cm^{-3} with $T=10^6-10^7$°K in scenario (b). For scenario (c) we used the combination of the two previous parameter sets. Values of B were delimited from the thermal flux N_o in SH 1.2-2, for every couple (n,T), by normalization of N_o with the point of maximum flux and minimum energy in the observational photon spectra. For the evaluation of the spectrum [10] of scenario (d) we sweped $n=10^{10}-10^{13}$cm^{-3}, $L=10^8-10^9$cm, $B=10^2-10^3$ gauss and $\varepsilon=10^{-3}-10$ V/cm; in this case two assumptions were worked out for the transport and photon emission regions respectively, first $n=10^{10}-10^{11}$ cm^{-3},$T=10^5-10^6$ °K with $n=10^9-10^{10}$ cm^{-3}, $T=10^6-10^8$ °K, and on the other hand $n=10^{10}-10^{12}$ cm^{-3}, $T=10^5-10^6$ °K with $n=10^{12}-10^{13}$ cm^{-3}, $T=10^4-10^5$ °K. For the acceleration efficiencies of the Fermi, Betatron and electric field acceleration processes in scenarios (a)-(c) we have required that the net energy change rate dE/dt>0 in eqs. [7] and [8] of paper SH 1.2-2. The mean acceleration time τ in eq. [6] is the free parameter of our analysis, however, we have restricted it to physically reasonably values quoted in the literature. Similarly we have proceeded for the selection of the three characteristic times of scenario (d): the characteristic time τ' of the injection rate in eq. [5] of SH 1.2-2, and the mean remain times τ_1 and τ_2 of particles in the trans-

---

**INAOE

* On leave for the Instituto Nacional de Astrofísica, Optica y Electrónica, A.P. 51, Z.P. 7200 - Puebla, México.

port and emission regions respectively. It should be noted that, although electric field acceleration in scenario (a) and neutral sheet acceleration in scenario (d) is basically the same process, in the former case we are adopting a thick geometry, while in the later energy losses in the acceleration volume are neglected (thin geometry), and the spectrum is derived in a quite a different form, by following particle trajectories in the electromagnetic field of the sheet is diffusion region. For the photon field we sweped from $\omega_{ph} = 10^{12}\text{-}10^{18}$ eV/cm^3.

2. Results. Low energy events and the impulsive phase of high energy events are better described within the frame of scenario (a) rather than with (d)(Figs.1-3). Acceleration in those events is better described by impulsive electric field acceleration in the context of thick geometries, while the dominant radiation process is the (IC) effect, even whithin the frame of the thin geometry of scenario (d). The range of accelerating electrid fields falls between $6.5\times10^{-3}\text{-}10^{-2}$ V/cm, whereas in scenario (d) higher fields are required (1-15) V/cm. Similarly, the adequate magnetic field strengths are 50-100 gauss, whereas in scenario (d) it is needed 400-500 gauss. Typical number densities are 10^{11} cm^{-3}, but 10^{10} cm^{-3} in the acceleration region with 10^{13} cm^{-3} in the emission region in scenario (d). Temperatures of 10^6 °K and photon fields > 10^{17}eV/cm^3 prevail in the source. Characteristic acceleration times are 0.03-0.06 s and much higher (30-50)s in scenario (d), where corresponding emission times are ∿80-100 s. Non-impulsive energy spectra of low and high energy events (usually associated to 2nd acceleration stage) are better described by stochastic acceleration from thermal energies, scenario (b), and radiation from (IC) than with injection from a preliminar acceleration phase within the volume of secondary stochastic acceleration scenario (c), in which case radiation appears from (BR). The acceleration efficiency in this kind of events must be very high (α=10-20 s^{-1}), while the corresponding acceleration times are quite shorter ∿ 0.002 s, but if the contribution of a first acceleration step is considered the acceleration efficiency turns to be lower. Typical parameters involved in these events are $n=10^{11}$cm^{-3}, $T\sim10^6$ °K, $B\sim50$ gauss, while ω_{ph} values $(10^{16}\text{-}10^{17})$eV/cm^3 are lower than in impulsive events. On the other hand, the global description of energy spectra composed of two different components (usually associated with two acceleration phases) is better assuming scenario (c) than with (b), in which case radiation from (IC) is dominant, with $\omega_{ph}\geq10^{17}$eV/cm^3, $\alpha \sim 1$ s^{-1}, τ=0.02s, $n=10^{11}$cm^{-3}, $T=10^6$ °K and B=50 gauss. Optimum fits to the observational spectra are sumarized in table 1.

3. Conclusions. From this study it can be infered that the scenario for the production of (X-γ) rays continum in solar flares may vary from event to event, however, it is possible in many cases to associate low energy events to impulsive acceleration, and the high energy phase of some events to stochastic acceleration. In both cases, flare particles seems to be strongly modulated by local energy losses. Electric field acceleration, associated for instance to neutral current sheets is a suitable candidat for impulsive acceleration. Finally we claim that the predominant radiation process of this radiation is the (IC) effect due to the local flare photon field.

TABLE 1

					ACCEL. PARAMETERS		FLARE PARAMETERS			BEST FITTING
EVENT	BEST SCENA-RIO	ACCEL. & LOSSES PROCESSES	RAD. PROC.	ω_{ph} (eV/cm^3)	ε(V/cm) $\alpha(s^{-1})$	τ(s) τ',τ_1,τ_2(s)	n(cm^{-3})	T(°K)	B(gauss)	(FIGS.1-6)
1-III- 970 X-RAYS 35-160 KeV ONE PHASE	(a)	EFA=electric field acceleration	IC	5×10^{17}	$\varepsilon=10^{-2}$	6×10^{-3}	10^{11}	10^6	90	EFA-IC
	(a)	BETA= betatron	IC	3×10^{16}	$\alpha=1$	0.3	10^{11}	10^7	100	
	(d)	NSA=neutral sheet acceleration	BR	-	$\varepsilon=10$	50,500,100	$10^{10}-10^{13}$	10^6	500	
30-III-1969 X-RAYS 28-254 KeV ONE PHASE	(a)	EFA	IC	10^{17}	$\varepsilon=6.5\times10^{-3}$	6×10^{-3}	10^{11}	10^6	50	EFA-IC
	(a)	EFA	BR	-	$\varepsilon=2$	10	10^{13}	2×10^5	100	
	(d)	NSA	IC	3×10^{17}	$\varepsilon=15$	50,2000,100	$10^{10}-10^{13}$	10^6	400	
4-III-1972 γ-RAYS 0.4-0.7 MeV 1st. PHASE	(a)	EFA	IC	10^{17}	$\varepsilon=5\times10^{-2}$	3×10^{-2}	10^{11}	10^6	50	EFA-IC
	(a)	BETA	IC	10^{16}	$\alpha=1$	0.2	10^{11}	10^7	120	
	(a)	BETA	BR	-	$\alpha=10$	1.	10^{11}	10^6	50	
	(d)	NSA	IC	2.5×10^{17}	$\varepsilon=1$	30,400,80	$10^{10}-10^{12}$	10^6	400	
4-III-1972 γ-RAYS 0.8-7MeV 2nd. PHASE	(b)	FERMI	IC	10^{17}	$\alpha=20$	2×10^{-3}	10^{11}	10^6	50	FERMI-IC
	(b)	FERMI	BR	-	$\alpha=1$	1.	10^{11}	10^6	50	
	(c)	(BETA-IC)-FERMI	BR	10^{16}	$\alpha=1$	5×10^{-2}	10^{11}	10^7	160	∿
30-III-1969 X-RAYS 28-254 KeV 2nd. PHASE	(b)	FERMI	IC	10^{16}	$\alpha=10$	2×10^{-3}	10^{11}	10^6	45	FERMI-IC
	(b)	FERMI	BR	-	$\alpha=0.5$	0.5	10^{11}	10^6	40	
	(c)	(EFA-IC)-FERMI	BR	10^{17}	$\varepsilon=10$	2×10^{-2}	10^{12}	10^6	100	∿
4-VIII-1972 γ-RAYS 0.4-7 MeV 1st. & 2nd. PHASE	(b)	FERMI	IC	10^{16}	$\alpha=10$	1.5×10^{-3}	10^9	10^7	45	∿
	(b)	FERMI	BR	-	$\alpha=1$	0.3	10^{10}	10^6	50	
	(c)	(EFA-IC)-FER	IC	10^{17}	5×10^{-2}	2.5×10^{-2}	10^{11}	10^6	50	
	(c)	(BETA-IC)-FERMI	IC	2×10^{17}	1.	0.02	10^{11}	10^6	50	(BETA-IC)-FERMI-IC
	(c)	(BETA-IC)-FERMI	BR	3×10^{16}	$\alpha=10$	7×10^{-2}	10^{11}	10^7	100	

References

Bai, T. and Ramaty, R., Solar Phys. 49, 343, 1976

Chung-Chih-Cheng, Space Sc. Rev. 13,3, 1972

Chupp, E. L. et al, Solar γ-X and EUV Radiation, IAU 68, 341, 1975

Crannel, C. J. et al, Ap. J. 223, , 1978

Frost, K. J. and Dennis, B. R., Ap. J. 165, 655, 1971

Jackson, W., Classical Electrodynamics, John Willey & Jons, Chap. 15, 1962

Kane, S. R. and Anderson, K.A., Ap. J. 162, 1003, 1970

Suri, A.N. et al, Solar Phys. 43, 415, 1975

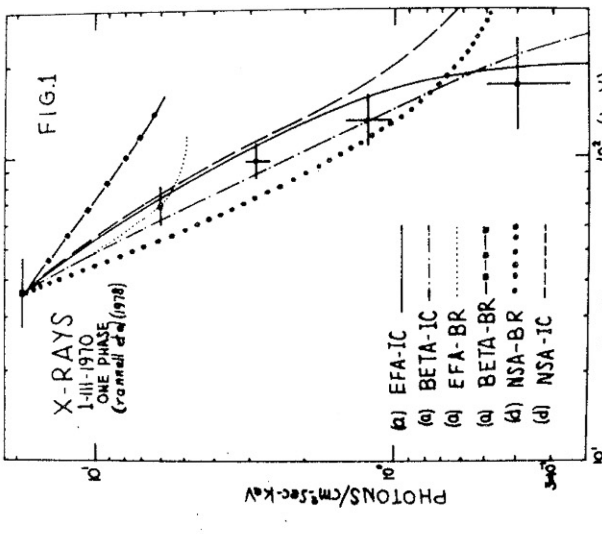

FIG.1

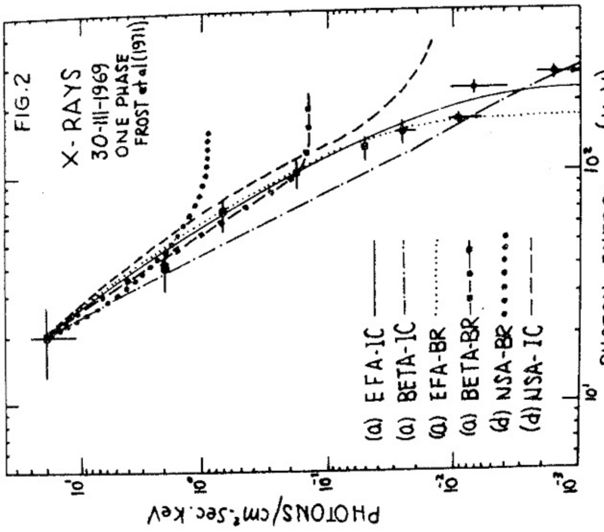

FIG.2

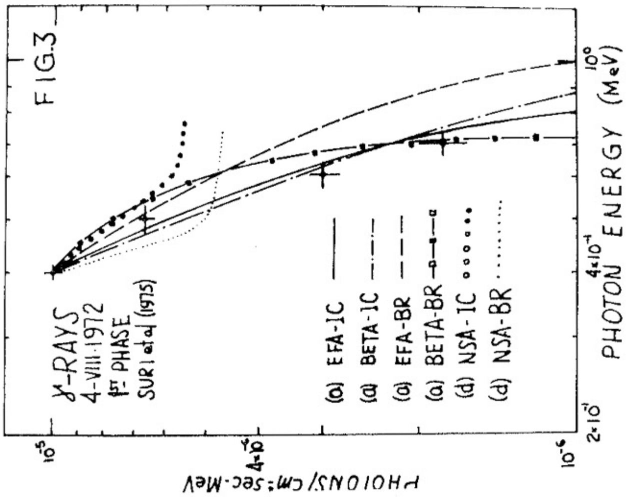

FIG.3

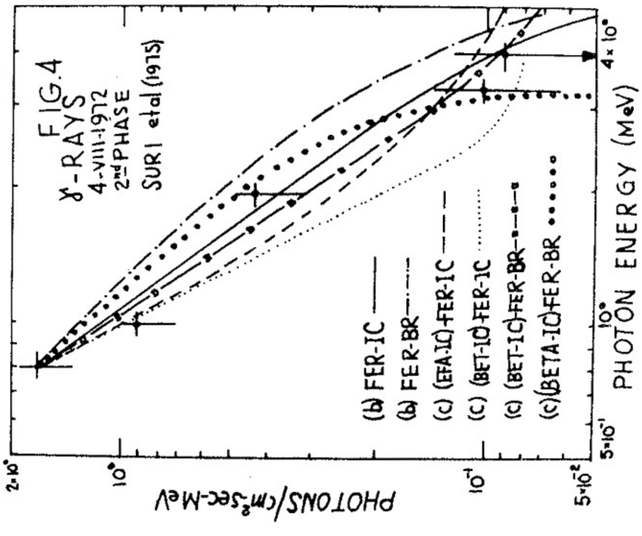

FIG.4

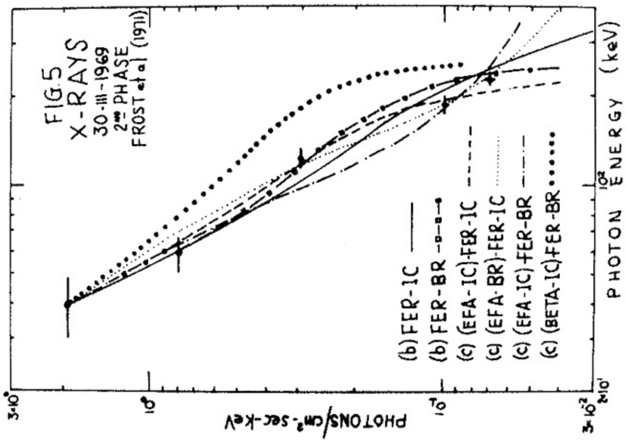

FIG.5

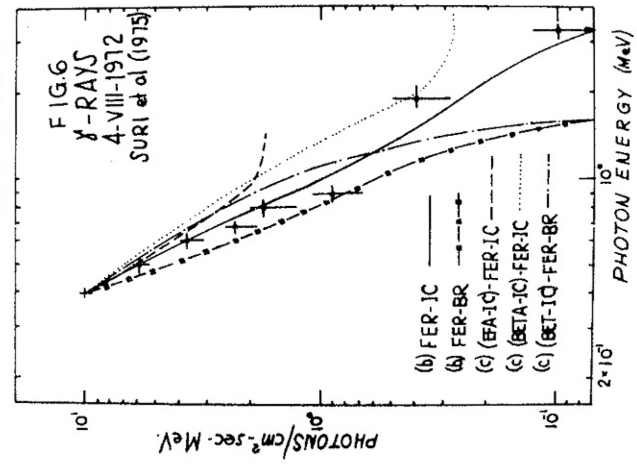

FIG.6